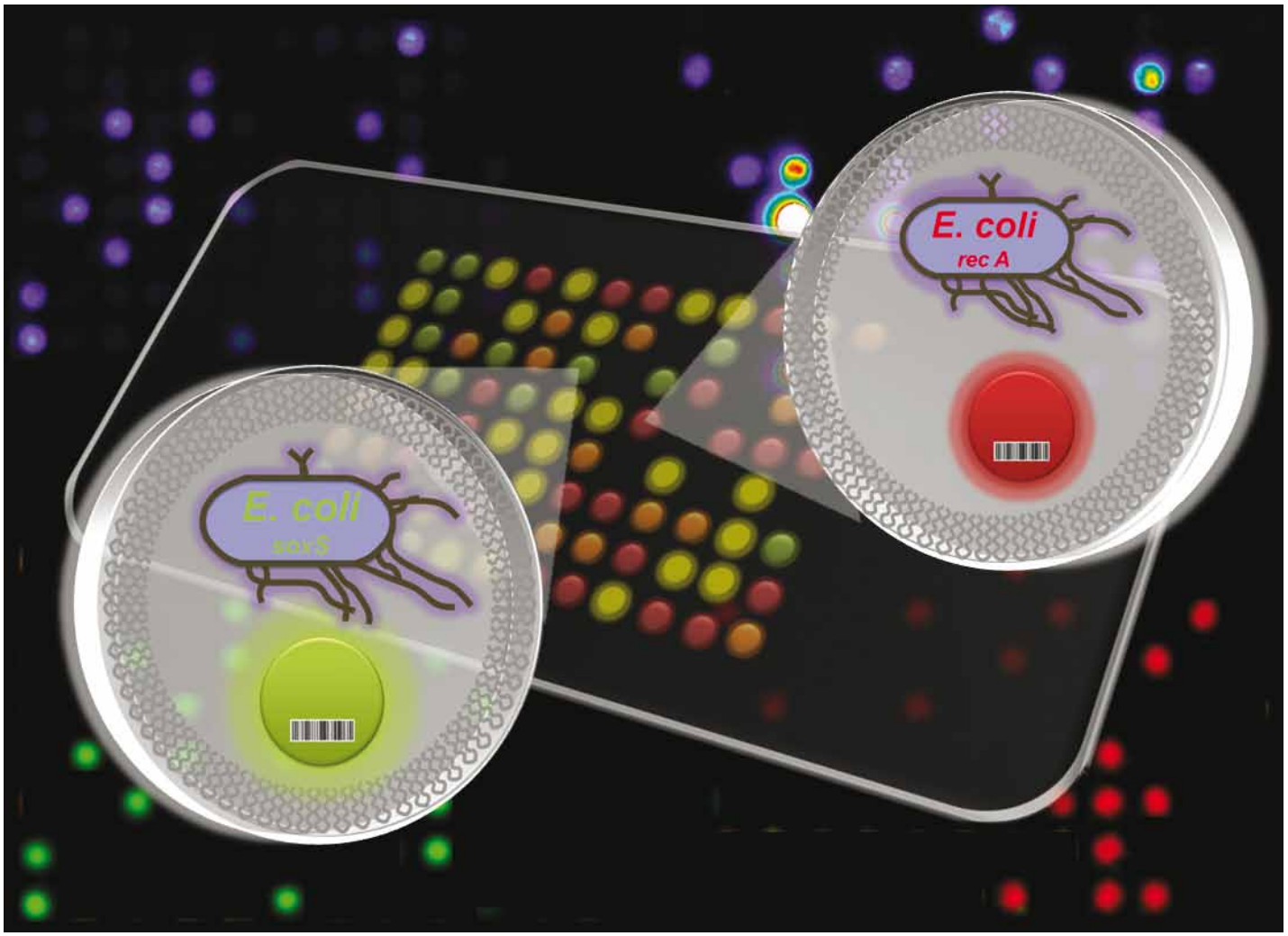

Featuring research from the group of Professor Man Bock Gu at Korea University, Seoul, Korea (South)

Title: Randomly distributed arrays of optically coded functional microbeads for toxicity screening and monitoring

A single alginate bead containing a type of stress-specific bioluminescent bacteria and a type of fluorescence microsphere as a self-identification code can have a dual function; to classify and measure toxicity and to facilitate the fabrication of the cell array chips by simply dropping the bead mixture on the chips.

As featured in:

See Gu et al., *Lab Chip*, 2010, **10**, 2695–2701.

Randomly distributed arrays of optically coded functional microbeads for toxicity screening and monitoring†

Joo-Myung Ahn,‡[a] Joong Hyun Kim,‡[b] Ji Hoon Kim[a] and Man Bock Gu*[a]

Received 8th April 2010, Accepted 11th June 2010
DOI: 10.1039/c004942e

We have successfully developed optically coded functional microbeads by co-encapsulating both bioluminescent reporter bacterial cells and fluorescent microspheres within a common alginate microbead. These microbeads harboring an individual self-identification code using fluorescent microspheres could be randomly scattered on any multi-well chip plate as long as the size of the microbeads are made to fit on it with the result that, since cell types are identified on the basis of fluorescent color, microbead arrays were fabricated without pre-designation of an individual well. As an example of this method, five different stress specific bioluminescent bacterial strains, each with a different optical code, were successfully implemented to make five different types of optically coded functional microbeads, with a speed of about 30 microbeads/min. Each functional microbead has a specific stress-specific bacterial strain and, as an identification optical code, one of five optical codes generated from fluorescence microspheres such as yellow, green, red, yellow + green, or no fluorescence. This final randomly scattered functional microbeads array biochip, with a fast fabrication of each chip at every 2 min, successfully demonstrated its ability in toxicity screening and monitoring for samples with a few examples for five different stress chemicals. This simple and fast, but not tedious and complicated procedure should be widely and practically used in making cell array chips for the monitoring of environmental toxicity, new-borne chemicals, pharmaceutical drugs and cosmic rays in the space station or spaceships in future.

Introduction

Cell-based toxicity screening methods have played important roles not only for human health but also for environmental protection. Especially, bacterial cell-based assays are being used for their rapidity in usage and easy manipulation for toxicological prescreening and environmental monitoring.[1] Rapid and clear enhancement in live/dead bacterial counting by incorporating a new non-invasive reporter system into the strains leads to great improvement, especially in a high-throughput assay. The naphthalene sensitive bioluminescent bacterial cell-based assay system[2] followed by heat-shock stress specific bioluminescent bacterial biosensors,[3] for example, provided the basis for a robust and sensitive reporter system for the novel development of chemical-[2] or stress-specific bioassays.[3,4] The production of newly designed substances and their uses has always been needed for the development of high throughput/multiplex toxicity screening chips, such as electrical circuit-based chip,[5] nylon membrane LuxArray,[6] optical fiber-based array,[7] and immobilization with agar-based array,[8] mostly focused to fabricate cell arrayed chips. However, the tedious and complicated procedures for preparing cell arrayed chips, in addition to the robustness and reliability of the chip, remain as challenges, especially for the practical adaptations in lead drug screening, environmental monitoring, or space station and spaceships in future, as well as for integration into an automated system. There have been previous studies reportig quantum dots[9] or different shapes of hydrogel[10] as possible coding methods for the contents in an individual moiety. Therefore, we present a bead-based toxicity screening method, consisting of randomly scattered arrays of optically coded functional microbeads bearing stress-specific bioluminescent bacteria and fluorescent microspheres coding a specific cell. In addition, the steps arraying the cells on a chip could be ever simplified and fast by only dropping the mixture of the microbeads randomly on the chip without any pre-designation. This newly elaborated and simplified method is considered to overcome the problems related to the fabrication of cell biochips, the tedious and complicated procedures, and robustness and reliability of the cell chip.

Methods and materials

Strains and cell culture

The genotypes and sources of five different stress-specific recombinant bioluminescent *E. coli* bacterial strains used in this study are listed in Table 1. The bioluminescent bacteria contained the backbone reporter system which is *Vibrio fischeri* or *Photorhabdus luminescens* promoter::*luxCDABE* genes with a stress-specific promoter constructed based either on pUCD615[11] or pDEW201,[12] respectively. DPD2794 and EBAlkA are specifically responsive to DNA damage[13] and alkylation-specific DNA damage[14] detection. DPD2540 is for

[a]*School of Life Sciences and Biotechnology, Korea University, Anam-dong, Seongbuk-gu, Seoul, 136-701, Republic of Korea. E-mail: mbgu@korea.ac.kr; Fax: +82-2-928-6050; Tel: +82-2-3290-3417*
[b]*BioNano Research Center, Korea Research Institute of Bioscience and Biotechnology (KRIBB), 111 Gwahangno, Yuseong-gu, Daejeon, 305-806, Republic of Korea*

† Electronic supplementary information (ESI) available: Supplementary note, Fig. S1 and Movie S1. See DOI: 10.1039/c004942e

‡ These authors contributed equally.

Table 1 Stress-specific bioluminescent bacterial strains and their corresponding fluorescent codes used in this study

Strain names	Plasmid/Host	Damaging stresses	Reference	Corresponding fluorescent codes
DPD2794	p*RecA*Lux/RFM443	DNA damage	Voller *et al.* (1997)[13]	Green
DPD2540	p*FabA*Lux/RFM443	Membrane damage	Belkin *et al.* (1997)[15]	No Fluorescence
DPD2511	p*KatG*Lux/RFM443	Oxidative damage (Hydroxyl radical)	Belkin *et al.* (1996)[25]	Orange
EBAlkA	pCH*alkA*Lux/RFM443	DNA damage (Alkylation)	Ahn *et al.* (2009)[14]	Red
EBSoxS	pBC*soxS*Lux/RFM443	Oxidative damage (Superoxide radical)	Kim *et al.* (2005)[16]	Yellow

membrane damage.[15] DPD2511 and EBSoxS are oxidative stress responsive, specifically to hydroxyl radical and superoxide radical,[16] respectively. Each strain was originally collected from a single colony on a Luria-Bertani (LB)–1.5% agar plate and grown in 5 ml LB medium (DIFCO) containing 50 μg ml^{-1} ampicillin (Sigma-Aldrich) in 15 ml falcon tubes (Corning) in a rotary incubator set at 37 °C and 200 rpm until the cell optical density reached early stationary phase (OD_{600} = ~0.8). For collecting concentrated cells, fresh media (100 ml) was inoculated with 2.5 ml of sub-cultured cells and this was then allowed to grow until the optical density reached 0.7 at 600 nm. At this cell density, the cells were collected by centrifugation at 12 000 rpm for 20 min at room temperature. After, supernatant was discarded and concentrated cells were stored at 4 °C until used.

Preparation of sodium alginate for electrostatic droplet generation

Sodium alginate (Sigma-Aldrich) 1.2 g was dissolved in 60 ml sterilized distilled water and 2% (w/v) of sodium alginate was prepared one day before making beads for matrix stabilization. Previously prepared centrifuged cells were resuspended using 9.7 ml of 2% sodium alginate to concentrate 10 times. And then 0.3 ml of surface unmodified fluorescent microsphere (3×10^9 fluorescent particles) (FluoSpheres 1 μm, Invitrogen) were added and mixed completely with vortexing for several minutes. In this study, we used three different fluorescent microspheres, blue-green, orange and red (Blue-Green F-13080, Orange F-18082 and Red F-18083, Invitrogen), and a mixed with fluorescent blue-green and red fluorescent microspheres which resulted in yellow fluorescence. Therefore, five optically coded microbeads can be generated by coding with three single fluorescence and one mixed fluorescence (yellow), in addition to no fluorescence.

Optically coded functional microbeads were generated by using the so-called electrospraying techniques.[17] Spherical microbead droplets were generated by extrusion of the solution containing sodium-alginate mixed with the cells and fluorescent microspheres through the connection of a 30.5 gauge needle and 40 cm sterilized silicone tube (A-06485-14 Cole-Parmer) using a syringe pump (HARVARD APPARATUS) with a 12 ml disposable plastic syringe (Henke-Sass, Wolf GmbH). The suspension of cells, fluorescent microsphere and sodium-alginate was forced out of the tip of the needle at a constant flow rate (2 ml h^{-1}), and droplets were formed by the action of both electrostatic and gravitational forces. Electrostatic potential was formed by connecting the negative electrode of a high voltage DC unit (Model ES30P 10W, HV power supply, Gamma high voltage, Florida) to the needle and positive aluminium electrode to grounding the gelling bath which was 50 ml of sterilized 2% (w/v) $CaCl_2$ (Sigma-Aldrich) solution. The negative electrode/needle tip was positioned 7 cm above the surface of the hardening solution. In order to investigate the effects of applied potential on bead sizes, the potential was varied in the range 2–8 kV during each set of experiments (see ESI†). After the formation of the beads, they were stirred in the same 2% (w/v) $CaCl_2$ solution for hardening for 60 min in order to assure the completion of the gelling process. After that period, the beads were rinsed and washed with LB media and were then stored in 50 ml centrifuge tubes (Corning, Falcon) for maintaining humidity in LB media at 4 °C in the dark until used.

Fabrication of optically coded functional microbead chips

Optically coded functional microbead chips were fabricated with black acrylic plates (holding 96-holes having 1 mm diameter). The 96-hole chips were made based on the computer-aided design (CAD) of holes on a plate of 4 cm × 2 cm × 1 mm (thickness), and cut using laser engraving and a cutting machine (Universal Laser Systems). Plates were 1.3 mm thick and 4 cm × 2 cm and have negligible auto-fluorescence. In order to sterilize each chip the following solutions were prepared and used in the following order on Laminar flow clean benches (Vision Sciences, Kyounggi, Rep. of Korea): (1) Deionized water (Millipore), (2) 70% ethanol, and (3) 100% ACS grade ethanol (Merck Co., USA) for the complete evaporation from the surface. Then, the chips were dried in Laminar flow clean benches under UV light for 30 min.

Each sterilized chip was placed in a 60 × 15 mm Petri-dish that was then filled with 5 ml LB medium (DIFCO Co., USA). Using sterilized glass Pasteur pipettes, a total mixture of 500 microbeads for each of the 5 different types of strains were randomly scattered onto the sterilized chip, and then the cover glass was slowly slipped onto the surface of the chip producing surface tension-based self filling of the microbeads into the holes and removal of unloaded extra microbeads (see ESI movie 1†). This pipetting and sealing procedure required only a few minutes. The chips covered up with a standard 22 × 40 mm cover glass (Marienfeld laboratory glassware, Germany) were kept at 4 °C in the dark until use.

Test chemicals and toxicity screening

Mitomycin C (MMC), 1-methyl-1-nitroso-*N*-methylguanidine (MNNG), paraquat, hydrogen peroxide (H_2O_2) and salicylic

acid (SA) (Sigma Aldrich) were selected to confirm the high throughput and multiplex toxicity screening features of the bead loaded chips.

The chemicals were prepared with distilled water except SA which was used with 50% ethanol. Before exposure to the test chemicals, optically coded functional microbead chips were taken out from 4 °C and incubated at 37 °C for 30 min to allow the cells to recover their sensing capabilities. After that, the cover glass which was placed on the top of the microbead chip was carefully removed by using forceps. The test sample was then gently poured into the Petri dish until the whole array was immersed in the sample solution (~300 μl). The microbead chip was placed in the dark box (Seolin Science Co., Rep of Korea) detection stage to measure bioluminescence every 10 min for 2 h. Time-resolved bioluminescent images of the chip were collected using a cooled charge-coupled device camera (Cooled CCD camera) (VersArray; Roper Scientific Inc., USA) with a constant focal plane and integration time (45 s). The light intensities were analyzed using MetaVue 5.0r6 (Universal Imaging Corp., USA) and expressed in a colorimetric manner for each pixel density. These data were transmitted to Microsoft office EXCEL 2007 (Microsoft Corp. USA) software to analyze bioluminescence induction.

Fluorescence measurements

Before exposure to the test chemicals, the fluorescence emission spectra of the optically coded microbead chip were determined using an *in vivo* multispectral imaging system (Maestro 2™, Cambridge Research & Instrumentation (CRI), Inc) in which the emission wavelength was extracted by using Maestro software 2.8.0 (Cambridge Research & Instrumentation, Inc). Green-to-red was detected by using the same filter settings. Green, orange and red fluorescence were excited at 455 nm (435 to 480 nm range), and detected through a 490 nm longpass emission filter. For acquisition settings, from 500 to 720 nm were scanned in 10 nm bands. The maximum emission wavelengths of green, orange and red fluorescence were detected at 540 nm, 570 nm and 620 nm, respectively. Also, for the bead containing two different fluorescent microspheres, the mixed fluorescence of green and red which resulted in yellow was detected and two peaks at weak 540 nm and 620 nm were shown (Fig. 1d). Imaging analysis was done on 1.3 megapixel images with 2/3 ROI (Region of Interest) in a 3.3 × 4.4 inches area.

Confocal Laser Scanning Microscope and its imaging software (Carl-Zeiss, LSM 5 Exciter) were used to determine fluorescent microsphere distribution in one microbead (Fig. 1c). The LSM was equipped with an EC Plan-Neufluor 10×/0.3M27_1 objective. Imaging was done by 3.20 μs pixel time and a 2.5 μm scaling size with 512 × 512 pixels. Red fluorescence was excited at 543 nm and was detected at 560 nm.

Results

Optically coded functional microbeads for toxicity screening

In brief, the presented method uses the encapsulation of two key components, *cells* of a bioluminescent bacterial strain for sensing specific stress and a specific type (color) of fluorescent *microspheres* as a self-identification code, into a single alginate bead to make one single functional *microbead*. Since each functional *microbead* contains a specific bacterial sensor and its

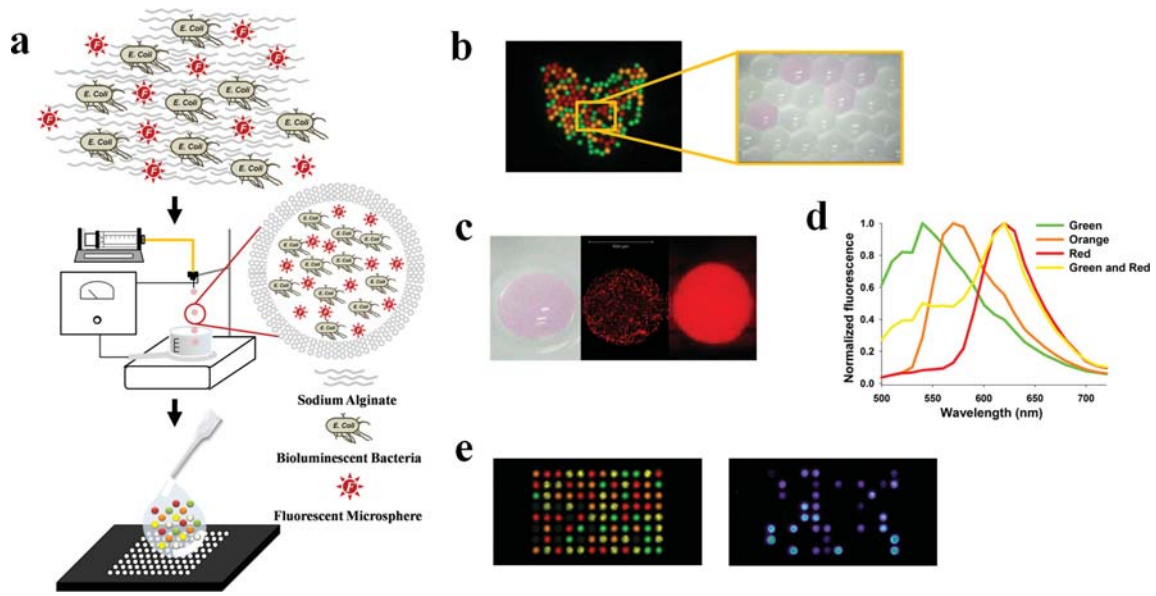

Fig. 1 Schematic of the optically coded functional microbead generation, the fabrication of microbead arrayed chips, and characteristics of fluorescent microspheres and microbeads. (a) A general scheme showing the components (stress-specific bioluminescent bacteria, fluorescent microspheres for coding the cells, and Na-alginate) used for making optically coded microbeads and the operation of electrospraying units to produce microbeads and the final format of the randomly scattered array chip fabricated by simply dropping a mixture of functional microbeads. (b) A fluorescence image showing the uniform size of the microbeads placed in a Petri dish. (c) A bright-light image and a fluorescence image of individual functional beads showing uniform distribution of fluorescent microspheres. (d) Fluorescent emission spectra of four distinct fluorescent microspheres. (e) Example of a fluorescence image (left) showing a clear difference from bioluminescent image (right) obtained from the same chip.

self-identification fluorescence *microsphere*, bioluminescence and fluorescence from a single *microbead* will indicate the toxicity level and its type of toxicity, respectively. In other words, a type of bacteria in a single bead among the randomly distributed bead mixture can be individually recognized and identified from the color of the designated self-identifying fluorescent microspheres (Fig. 1a). These functional fluorescent/luminescent beads were generated by the electrospraying method[17] which is simple and fast in fabricating the microbeads uniformly (Fig. 1b). After the size optimization in terms of bacterial cell concentrations, infusion rates, and electric voltages, the generation of microbeads was successfully conducted and confirmed with uniform fluorescent microsphere distribution in a single alginate bead as well (Fig. 1c). The electrospin method for preparing particles is described in the ESI†.

In order to show the effective features of the bead-based toxicity screening method, five distinguishable microbeads were prepared using four different fluorescent microspheres (green, orange, red and yellow) to indicate five different stress-specific bioluminescent bacterial strains used as a model in this study. The bacterial strains are DPD2794 coded with green, DPD2511 with orange, EBAlkA with red, EBSoxS with yellow and DPD2540 coded with no fluorescence (without fluorescent microspheres), which are responsive for DNA damage, hydroxyl radical oxidative damage, alkylation DNA damage, superoxide radical oxidative damage, and membrane damage, respectively (Table 1). Using a multispectral imaging system, the emission spectra were measured for four different fluorescent microspheres, indicating that their spectra are distinct and separated (Fig. 1d). Equal numbered bead mixtures were easily and quickly placed and randomly distributed on 1.3 mm thickness of custom made 96 micro-well plastic chip (4 cm × 2 cm) by Pasteur pipette (See ESI movie 1†). Once the fluorescent image maps of the bead-based chip were obtained, we were able to clearly differentiate fluorescent emission of each bead from the cell bioluminescence (Fig. 1e). As can be seen, therefore, its set up procedure and method for generating beads and making the randomly distributed microbead chips, was very simple and fast, especially without any special attention to place a certain microbead in a certain spot on the chip, which is superior to other previously studied methods.

Stress-specific responses of functional microbeads

The response of each type of functional microbead was characterized based on the images of the bioluminescence emission at 120 min after exposure by using pixel analysis for time-course changes in bioluminescence in response to LB only (blank) and

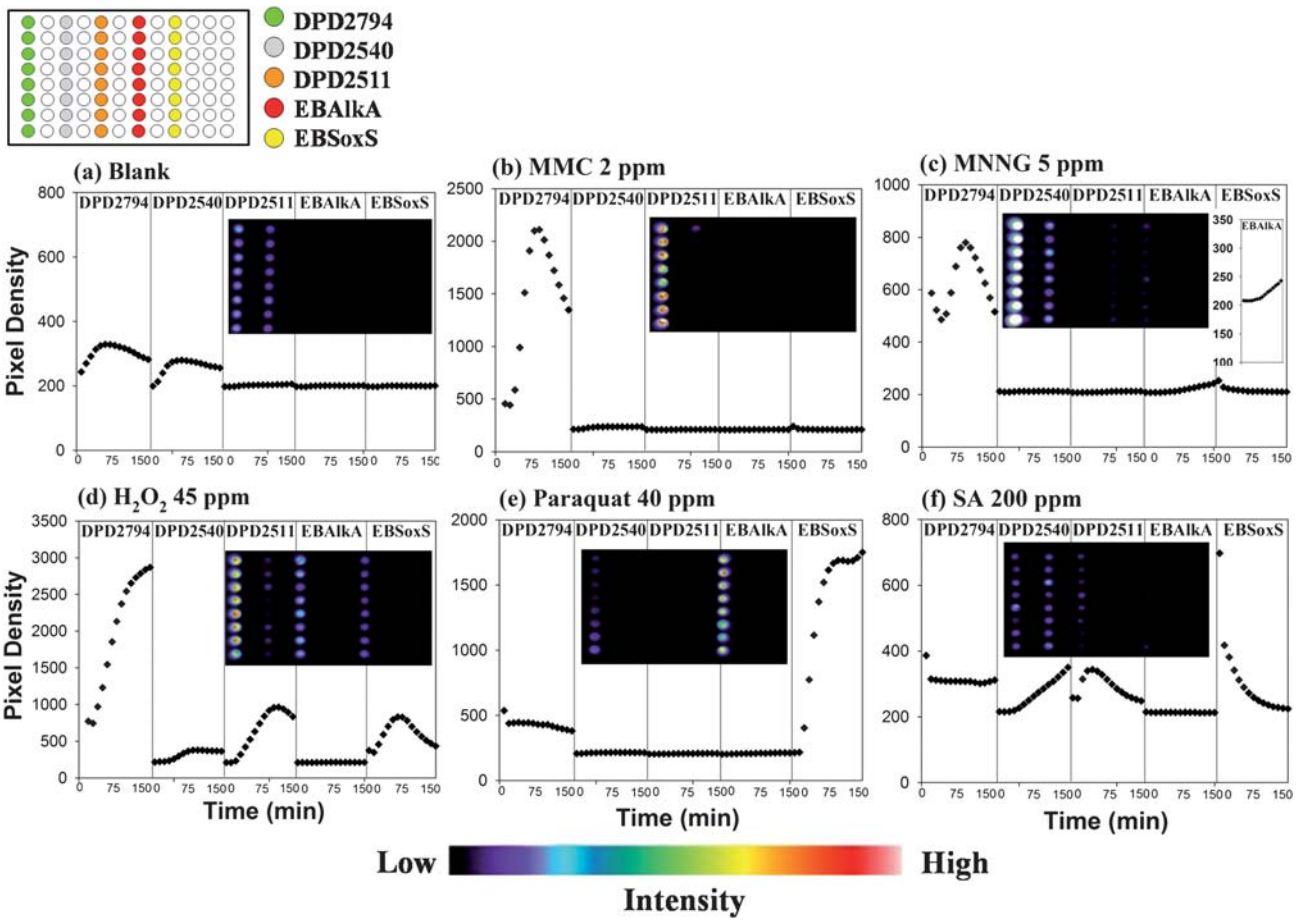

Fig. 2 The responses of the optically coded functional microbeads were characterized based on the images of the bioluminescence emission at 120 min after the exposure. (a) LB media as a blank, (b) mitomycin C (MMC), (c) 1-methyl-1-nitroso-n-methylguanidine (MNNG), an enlarged graph showing clear response of EBAlkA, (d) hydrogen peroxide (H_2O_2), (e) paraquat, and (f) salicylic acid (SA).

five different chemicals (Fig. 2). The bioluminescent response to the blank was considered to be the basal level; DPD2794 coded with green and DPD2540 coded with no fluorescence showed high bioluminescence compared to the basal level, 329 and 279, respectively (Fig. 2a). MMC is a direct DNA damaging agent by covalently binding to the minor groove of DNA, thus preventing the separation needed for DNA replication.[18] Only DNA damage responsive strain which is DPD2794 coded with green microspheres was brightened at the first lane from the left, taken at 40 min after exposure (Fig. 2b). MNNG causes DNA alkylation damage.[19] It caused high induction of DPD2794 and also caused EBAlkA (coded with red) induction which is clearly seen with the enlarged pixel analysis (Fig. 2c). Hydrogen peroxide produced hydroxyl radicals that cause oxidative stress inducing direct oxidative stress response,[20] and DPD2511 and EBSoxS strains are induced. However, this induction intensity was decreased about an hour due to oxidative defense mechanism in *E. coli*.[21] Also, DPD2794 strain induced by indirect oxidative DNA damage response is also occurred significantly from 40 min after the exposure (Fig. 2d). Paraquat which produces superoxide radical should be a strong base that can react with protons from a variety of compounds. Paraquat easily penetrates into cells and induces a cyclic one-electron reduction of molecular oxygen to the superoxide radical using the oxidation of redox enzymes present within the cell.[20] Therefore, it was chosen to measure superoxide-induced oxidative response in this study. As characterized previously,[16] EBSoxS strain was clearly seen to be induced from 30 min after exposure (Fig. 2e). Salicylic acid (SA) which causes an uncoupling of oxidative phosphorylation and induces transcription of heat-shock and membrane damage sensitive genes within *E. coli*.[22] The effect of salicylic acid can be observed initially on oxidative stress, and so EBSoxS strain was suddenly increased (0 min) and DPD2511 also induced at 40 min (Fig. 2f). This oxidative stress also triggered induction of DPD2540, which is responsive to conditions that lead to fatty acid limitation, such as membrane damage.[23] In summary, certain beads show significant bioluminescent induction in response to a specific model chemical in a promoter-dependent manner, while other beads have no distinct bioluminescence emission.

Randomly scattered arrays of optically coded functional microbeads

As a practical example of how this bead chip can be utilized, Fig. 3 shows the response snapshots of bioluminescence and fluorescence from randomly distributed beads on the chip after 2 h of exposure to the model substances. As can be seen clearly in Fig. 3b and c, the patterns of the bioluminescence perfectly matched with the fluorescence patterns. The bioluminescence image (Fig. 3b) at the very left column for MMC is well matched with the corresponding fluorescence image (Fig. 3c) of the microbead spots only containing DPD2794 cells which are coded by green color fluorescence. Except for a few spots, an excellent match of the luminescence pattern was also obtained for 1-methyl-1-nitroso-*N*-methylguanidine (MNNG) (10 ppm) with EBAlkA. A few bioluminescence microbead spots not matched with the image of the red fluorescence spots in the 2nd column is due to microbeads that contain the DPD2794 strain coded with green (not red). This exception is the result (the 2nd column from

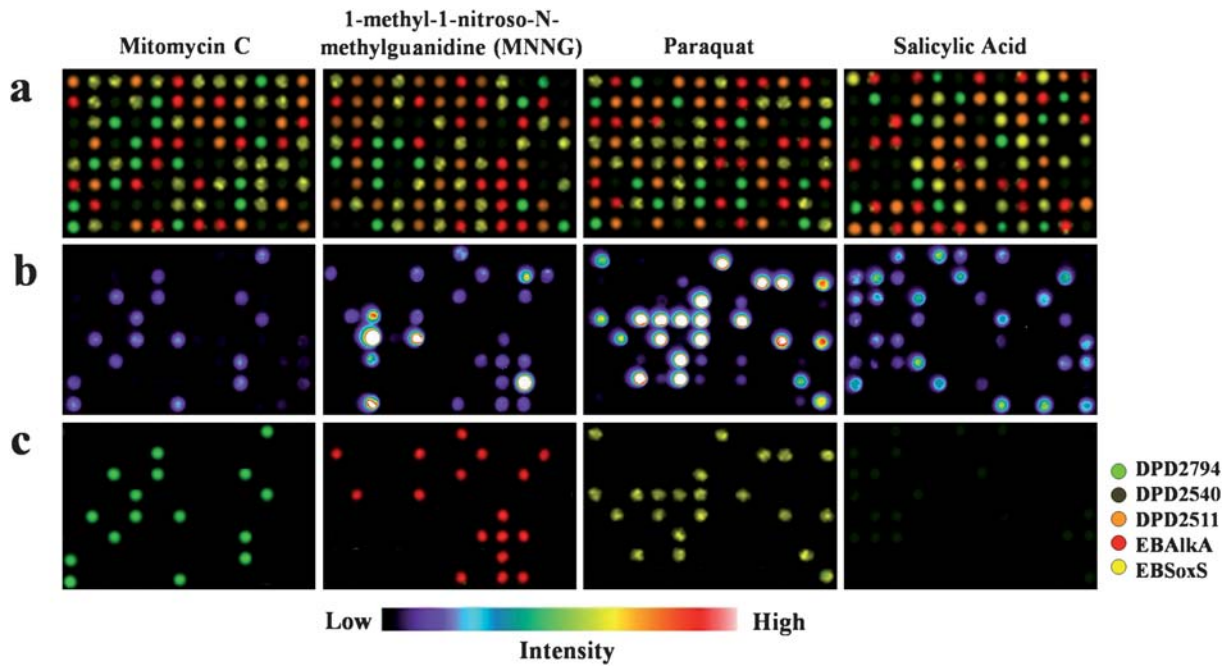

Fig. 3 An example of high throughput and multiplex toxicity screening using randomly scattered functional microbead chips for four different chemicals. All snapshots of bioluminescence/fluorescence images were taken after 120 min of exposure of the chip to the chemicals. (a) A complete fluorescent image showing the identification of all microbeads randomly scattered on the chip. A distinct fluorescent color from each microbead indicates the identification of a specific bioluminescent bacterial strain immobilized in the same microbead. (b) The bioluminescence images and (c) the corresponding fluorescent images responsive to specific chemicals, from left to right in the following order: mitomycin C, 1-methyl-1-nitroso-*N*-methylguanidine (MNNG), paraquat, and salicylic acid, respectively.

the left) of MNNG (10 ppm) causing responsiveness of not only the red-coded EBAlkA strain but also the green coded DPD2794 cells as well. Paraquat (40 ppm) is known to cause superoxide radical oxidative stress in the cells, and EBSoxS strain can be responsive to this chemical. Therefore, the image of the bioluminescence microbead spots containing only EBSoxS strain appeared to be matched to yellow fluorescent image spots which should be likely due to its coding to EBSoxS strain for Paraquat (the 3rd column from left). Salicylic acid (SA) (200 ppm) (the first column from the right) is known to cause oxidative stress initially, and then gradually trigger membrane damage.[22] The image of the bioluminescence microbead spots at 120 min after exposure is from only a membrane damage sensitive strain DPD2540 which was not coded with any fluorescent microspheres, and thus not fluorescence coded, which resulted in auto fluorescence appearing as pale green but easily distinguishable. Moreover, the bimodal toxicity[24] of hydrogen peroxide causing oxidative and DNA damage simultaneously could also be classified successfully in this system (see ESI Fig. 1†). This demonstration of a functional bead-based biochip system clearly describes the distinct features of the design for the high throughput and multiplexed toxicity screening by simply dropping the mixture of the functional microbeads randomly on a chip.

Discussion

The optically coded functional microbead system described here has a few clear advantages over the previously studied cell-based assay: (i) the method for generating the beads is fast, simple, and robust due to the use of well-known immobilization material, sodium-alginate, and the electrospraying technique. This means that these optically coded bioluminescent microbeads can be generated quickly without any specific devices such as micro-size syringe pump or micro-, nano-scale channels, (ii) the generation of randomly distributed bead-based chips or bead-based capillary columns can be fabricated on any plates or in capillary columns in an easy and rapid manner without any special equipment for the array of cells or beads in specific, designated wells. In fact, the most complicated step in making the cell array chips is the allocation of correctly matched cells in a designated location. This method uses the self-identification code with different fluorescent beads. Even though there is heavy spectral overlap among those fluorescence spectra, the distinction was clearly made by appointing a certain wavelength for each type of microbead when the fluorescence is scanned. In addition, these optically coded functional microbeads required smaller amounts of cells due to its small microbead volume, and resulted in faster response time than the other immobilization methods. These features may allow us to fabricate a single bead-based small capillary-type needle, which could be fitted in any of the very narrow spaces usually required in the space station or spaceships in future. The response data obtained from this system can be clearly interpreted based on a yes–no paradigm, and the bioluminescence signal can be interpreted as a certain concentration if the sample contains a single material, as the bioluminescence response signal is dose-dependent.

In summary, we have demonstrated the versatile functionalities of a toxicity screening method, in terms of its simplicity, robustness and rapidity in preparing the randomly distributed microbeads-based chip for screening toxicity. This is achieved by combining 3 functional materials into one microbead such as a toxicity sensing bacterial strain and a specific type of fluorescent microsphere fabricated into alginate beads. Since the fabrication of the microbeads is straightforward and reproducible, in addition to robustness of the beads for long term storage (at least one month stability shown to date), the presented formulation is expected to be widely and practically adopted for preparing cell-based array chips for any types of cells, with literally unlimited combinations of fluorescent microspheres for the screening of a lead drug, the monitoring of environmental toxicity, and the toxicity and risk assessment of the cosmic rays in the space station or spaceships in future.

Acknowledgements

We thank to Dr Paul Todd at Techshot, Inc., USA, for his critical review and comments on this manuscript before submission. We appreciate Mr Ee Taek Hwang in Korea University for his help in operating electrospraying units. This study was supported in part by the Eco-technopia 21 project program of the Ministry of Environment (Project # 091-071-066), and Basic Science Research Program through the National Research Foundation of Korea (NRF) funded by the Ministry of Education, Science and Technology (Project # 2010-0011283). The authors are grateful for the support.

References

1 K. Yagi, *Appl. Microbiol. Biotechnol.*, 2007, **73**, 1251–1258.
2 J. M. H. King, P. M. Digrazia, B. Applegate, R. Burlage, J. Sanseverino, P. Dunbar, F. Larimer and G. S. Sayler, *Science*, 1990, **249**, 778–781.
3 T. K. Van Dyk, W. R. Majarian, K. B. Konstantinov, R. M. Young, P. S. Dhurjati and R. A. Larossa, *Appl. Environ. Microbiol.*, 1994, **60**, 1414–1420.
4 T. K. Vandyk, A. A. Gatenby and R. A. Larossa, *Nature*, 1989, **342**, 451–453.
5 M. L. Simpson, G. S. Sayler, B. M. Applegate, S. Ripp, D. E. Nivens, M. J. Paulus and G. E. Jellison, *Trends Biotechnol.*, 1998, **16**, 332–338.
6 T. K. Van Dyk, E. J. DeRose and G. E. Gonye, *J. Bacteriol.*, 2001, **183**, 5496–5505.
7 Y. Kuang, I. Biran and D. R. Walt, *Anal. Chem.*, 2004, **76**, 2902–2909.
8 J. H. Lee, R. J. Mitchell, B. C. Kim, D. C. Cullen and M. B. Gu, *Biosens. Bioelectron.*, 2005, **21**, 500–507.
9 M. Y. Han, X. H. Gao, J. Z. Su and S. Nie, *Nat. Biotechnol.*, 2001, **19**, 631–635.
10 J. E. Meiring, M. J. Schmid, S. M. Grayson, B. M. Rathsack, D. M. Johnson, R. Kirby, R. Kannappan, K. Manthiram, B. Hsia, Z. L. Hogan, A. D. Ellington, M. V. Pishko and C. G. Willson, *Chem. Mater.*, 2004, **16**, 5574–5580.
11 P. M. Rogowsky, T. J. Close, J. A. Chimera, J. J. Shaw and C. I. Kado, *J. Bacteriol.*, 1987, **169**, 5101–5112.
12 T. K. Van Dyk and R. A. Rosson, *Methods Mol. Biol.*, 1998, **102**, 85–95.
13 A. C. Vollmer, S. Belkin, D. R. Smulski, T. K. VanDyk and R. A. LaRossa, *Appl. Environ. Microbiol.*, 1997, **63**, 2566–2571.
14 J. M. Ahn, E. T. Hwang, C. H. Youn, D. L. Banu, B. C. Kim, J. H. Niazi and M. B. Gu, *Biosens. Bioelectron.*, 2009, **25**, 767–772.
15 S. Belkin, D. R. Smulski, S. Dadon, A. C. Vollmer, T. K. Van Dyk and R. A. Larossa, *Water Res.*, 1997, **31**, 3009–3016.
16 B. C. Kim, C. H. Youn, J. M. Ahn and M. B. Gu, *Anal. Chem.*, 2005, **77**, 8020–8026.
17 J. P. Halle, F. A. Leblond, J. F. Pariseau, P. Jutras, M. J. Brabant and Y. Lepage, *Cell Transplant.*, 1994, **3**, 365–372.
18 V. S. Li and H. Kohn, *J. Am. Chem. Soc.*, 1991, **113**, 275–283.

19 R. Saffhill, G. P. Margison and P. J. Oconnor, *Biochim. Biophys. Acta-Rev. Cancer*, 1985, **823**, 111–145.
20 B. Demple, *Annu. Rev. Genet.*, 1991, **25**, 315–337.
21 B. C. Kim and M. B. Gu, *Process Biochem.*, 2007, **42**, 392–400.
22 K. Shirasu, H. Nakajima, V. K. Rajasekhar, R. A. Dixon and C. Lamb, *Plant Cell*, 1997, **9**, 261–270.
23 S. H. Choi and M. B. Gu, *Environ. Toxicol. Chem.*, 2001, **20**, 248–255.
24 J. H. Min, E. J. Kim, R. A. LaRossa and M. B. Gu, *Mutat. Res., Genet. Toxicol. Environ. Mutagen.*, 1999, **442**, 61–68.
25 S. Belkin, D. R. Smulski, A. C. Vollmer, T. K. VanDyk and R. A. LaRossa, *Appl. Environ. Microbiol.*, 1996, **62**, 2252–2256.